*J. Fluid Mech.* (1991), *vol.* 227, *pp.* 407–427
*Printed in Great Britain*



# Flame balls stabilized by suspension in fluid with a steady linear ambient velocity distribution

By J. BUCKMASTER[1] AND G. JOULIN[2]

[1] Department of Aeronautical and Astronautical Engineering, University of Illinois, Urbana, IL 61801, USA

[2] CNRS, Poitiers, France

(Received 10 April 1990 and in revised form 20 November 1990)

The ignition of lean $H_2$/air mixtures under microgravity (μg) conditions can lead to the formation of spherical premixed flames (flame balls) with small Péclet number (*Pe*). A central question concerning these structures is the existence of appropriate stationary stable solutions of the combustion equations. In this paper we examine an individual flame ball that is suspended in a fluid whose velocity far from the flame is steady and varies linearly in space. Detailed results are obtained for simple shear flows and simple straining flows, both axisymmetric and plane.

Convection enhances the flux of heat from the flame and the flux of mixture to the flame, but because the Lewis number (*Le*) is less than unity the relative impact on the former is greater than on the latter. Consequently, there is a net loss of energy from the flame to the far field, and if large enough this will quench the flame. For values of shear or strain less than the quenching value there are two possible stationary solutions, but one of these is unstable to spherically symmetric disturbances of the flame ball. The radius of the other solution is unbounded as *Pe* goes to zero. Examination of a class of three-dimensional disturbances reveals no additional instability when the energy losses are due only to convection, but sufficiently large flame balls are unstable when volumetric heat losses from radiation are accounted for. This last result is in agreement with previous results that have been obtained for zero *Pe*, albeit with inadequate accounting for the flow field generated by the perturbations.

## 1. Introduction

When very lean $H_2$/air mixtures are ignited, Turing instabilities cause fragmentation of the flame. (These are instabilities that arise because the Lewis number *Le* differs from unity. Here *Le* is small and the Turing instability is the well-known cellular instability of premixed flames (Williams 1985).) At Earth's gravity small flame caps 4 mm or so in diameter are generated, and these rise at steady speed because of buoyancy effects and appear to have permanent form (Lewis & von Elbe 1987). Under microgravity (μg) conditions spherical flames (flame balls) are observed with diameters between 1 and 2 cm (Ronney 1990). Whether or not these have permanent form is unresolved by drop-tower experiments (Ronney 1990) because of the short test times (2.2 s), but recently they have been seen in flight tests (Keplerian trajectory) for up to 15 s (P. Ronney, private communication) and we believe that their existence is no longer in doubt. This paper is concerned with the structure and stability of such flames.

The ignition process and subsequent flame evolution generate an unsteady flow field, but the flame balls are carried along by this flow and their spherical shape suggests that convection effects are small. Thus a natural starting point is to neglect convection entirely and seek stationary flame solutions with a quiescent far field. This was first done by Zeldovich (see Zeldovich *et al.* 1985) motivated by the 1 g observations. The equations, which we shall describe later, then admit solutions in which the gas velocity is zero everywhere; these are curious creatures, premixed flames in which the only fluxes are diffusional, but they do no violence to the physics.

Not surprisingly, the solutions constructed by Zeldovich are unstable. The hot burnt gas and the flame which encloses it can act as an ignition source for the surrounding mixture, increasing the volume of burnt gas. Inward collapse is also possible, but intuitively less obvious. Thus if we are to understand the experimental observations it is necessary to identify stabilizing mechanisms.

In Buckmaster, Joulin & Ronney (1990) it is shown that volumetric heat losses associated with radiation can stabilize flame balls. Specifically, if the losses are too large the flame will be quenched, but for losses less than the quenching value there are two solutions (figure 1) and, although the small-flame solution is unstable to one-dimensional disturbances and part of the large-flame branch is unstable to three-dimensional disturbances, there is an interval of large-flame solutions that are stable.

Buckmaster *et al.* (1990) is only concerned with losses from the hot gases near the flame. In Buckmaster, Joulin & Ronney (1991) it is shown that losses from the relatively cool gases far from the flame also can stabilize, although the stability picture is modified with the neutral stability point for one-dimensional disturbances moving to the upper branch (figure 2). (In our analysis, the concept of 'near' and 'far' has a precise mathematical meaning which we shall define in due course.)

Although there is evidence that radiation losses are significant for flames in the near-limit mixtures that support flame balls, left unresolved in all of this work is whether or not the experimental heat losses have the correct magnitude. They are difficult to estimate.

In the present paper we shall consider another way in which energy can be extracted from a flame ball. The flame is a source of heat and for fixed source strength convection will generate additional heat losses which, when the Péclet number, $Pe$, (based on mass diffusion) is small, are proportional to $(Pe/Le)^{\frac{1}{2}}$. At the same time it is a sink of mixture and for fixed sink strength there will be an additional flux proportional to $Pe^{\frac{1}{2}}$. These increments are not in balance since for the mixtures of interest $Le < 1$ (Lewis numbers of 0.2–0.3 are typical of lean $H_2$/air mixtures) so that the incremental thermal enthalpy loss is greater than the incremental chemical enthalpy gain. Thus the source strength must adjust to restore the necessary energy balance, and the flame temperature will drop, just as it does when radiation losses are present.

Consider a flame ball located in a flow that is non-uniform on a scale much larger than the flame radius. Then the flame ball will be swept along by the flow with insignificant lag, and in a flame-fixed frame the gas velocity in the neighbourhood of the ball will be a linear function of position vanishing at the ball itself. These are the flows that we shall consider, with detailed results for linear shear flows and linear straining flows. The Péclet number associated with these flows is defined later.

We conclude this section with a brief description of the layout of the paper.

Section 2 is concerned with the mathematical formulation and the specification of scaled non-dimensional variables. A key feature of our model is the flame-sheet approximation, valid when the activation energy characterizing the Arrhenius'

kinetics is very large. A non-dimensional activation energy $\theta$ ($\theta \gg 1$) then becomes the key parameter of the problem, defining the length- and timescales. A *near-field* is defined on the scale of the flame-ball radius, and a *far-field* on the scale of $\theta \times$ radius.

Section 3 examines unsteady spherical flame balls. These evolve on the timescale $\theta^2 t_{\rm diff}$, where $t_{\rm diff}$ is the diffusion time based on the flame radius. Solution of the near field leads to the fundamental equation for the radius $\bar{r}_*$,

$$1 = \bar{r}_* \exp\left[\frac{h - \frac{1}{3}\bar{r}_*^2 F_{\rm b}}{2\bar{T}_{\rm b}^2}\right], \tag{1.1}$$

where $F_{\rm b}$ is a constant determined by radiation losses in the burnt gas, $\bar{T}_{\rm b}$ is essentially the flame temperature, and $h$ is a function of the slow time $t/\theta^2 t_{\rm diff}$ determined from matching with the far field. Steady solutions are constructed ($h =$ constant) by examining far fields controlled by linear flows, and then

$$h \propto -\omega^{\frac{1}{2}}(1-(Le)^{\frac{1}{2}})\,\bar{r}_*, \tag{1.2}$$

where $\omega$ is the applied velocity gradient. A one-dimensional stability analysis is carried out by constructing infinitesimal unsteady perturbations of $h$ generated by the far field.

Section 4 considers perturbations to the flame sheet in the form of surface harmonics, and so deals with the three-dimensional stability question. These perturbations evolve on the timescale $\theta t_{\rm diff}$ and this, being much faster than the one-dimensional timescale, complicates the discussion.

## 2. Mathematical formulation

The governing equations that we shall solve are

$$\rho C_p \frac{{\rm D}T}{{\rm D}t} = \lambda \nabla^2 T + QB\,{\rm e}^{-E/2RT_*}\delta - f(T), \tag{2.1a}$$

$$\rho \frac{{\rm D}Y}{{\rm D}t} = \rho D \nabla^2 Y - B\,{\rm e}^{-E/2RT_*}\delta, \tag{2.1b}$$

$$\frac{\partial \rho}{\partial t} + \nabla\cdot(\rho \boldsymbol{v}) = 0, \quad \rho \frac{{\rm D}\boldsymbol{v}}{{\rm D}t} = -\nabla p + \mu[\nabla^2 \boldsymbol{v} + \tfrac{1}{3}\nabla(\nabla\cdot\boldsymbol{v})], \tag{2.1c, d}$$

$$\rho T = \rho_{\rm f} T_{\rm f}, \tag{2.1e}$$

with boundary conditions

$$\left.\begin{array}{c} \rho \to \rho_{\rm f}, \quad T \to T_{\rm f}, \quad Y \to Y_{\rm f} \quad \text{as} \quad r \to \infty \\ v \text{ a specified linear function of position.} \end{array}\right\} \tag{2.2}$$

These are, for the most part, the usual equations for low-Mach-number combustion (Williams 1985). Thus $p$ is the hydrodynamic pressure and is not to be confused with the thermodynamic pressure that would normally appear in the equation of state. This latter quantity is constant so that the equation of state reduces to Charles's law, (2.1*e*).

The chemistry is modelled by a one-step irreversible process

$$Y \to \text{products}$$

at a rate proportional to $Y\mathrm{e}^{-E/RT}$,

where $E$ is the activation energy, assumed to be a large quantity. More precisely, our entire discussion is an asymptotic treatment valid when

$$\frac{E}{RT_*} \to \infty, \tag{2.3}$$

where $T_*$ is the flame temperature. In this limit, reaction is confined to a vanishingly thin flame sheet (where the temperature is $T_*$), and is equivalent to a Dirac $\delta$-function whose strength is proportional to $\exp(-E/2RT_*)$ (Buckmaster & Ludford 1983). This is the origin of the sink term in (2.1 *b*) ($B$ is a constant).

Consumption of the mixture $Y$ generates heat. In a spatially homogeneous situation with no losses ($f \equiv 0$) the associated rise in temperature is given by

$$\delta T = -\frac{Q}{C_p}\delta Y,$$

so that $Q$ is a measure of the chemical enthalpy. This is the origin of the positive source term in (2.1 *a*).

The function $f(T)$ is a volumetric heat-loss term that represents radiation losses. This mechanism is discussed in Buckmaster *et al.* (1990) but is included here because our three-dimensional stability analysis is done without adopting the constant-density model used in the earlier work. As there, it is assumed that $f$ is non-zero only in the hot burnt gas.

Bulk viscosity is neglected and the transport coefficients $\lambda$, $\rho D$, and $\mu$, together with $C_p$, are constants.

If we integrate (2.1 *a*, *b*) across the flame sheet the following jump conditions are generated:

$$B\mathrm{e}^{-E/2RT_*} = \rho D\left[\frac{\mathrm{d}Y}{\mathrm{d}n}\right] = -\frac{\lambda}{Q}\left[\frac{\mathrm{d}T}{\mathrm{d}n}\right], \tag{2.4}$$

where $n$ is the distance measured along the outer normal to the sheet and the square bracket denotes a jump, unburnt-side values minus burnt-side values. Note that the strength of the $\delta$-function, and therefore the magnitude of these gradient jumps, is very sensitive to changes in $T_*$ when $E$ is large. A change in $T_*$ of magnitude $O(T_*(RT_*/E))$ generates order of magnitude changes in the gradients and the overall solution. As we shall see, small Péclet numbers can generate changes in $T_*$ of this size via the mechanism described in §1, and therefore can have a significant impact on the combustion field.

Finally, we note that implicit in the asymptotic treatment of the chemical kinetics is the condition

$$Y \equiv 0 \quad \text{in the burnt gas.} \tag{2.5}$$

### 2.1. *The Zeldovich solution*

Equations (2.1) admit a steady, spherically symmetric solution for which $v \equiv 0$. When there are no radiation losses ($f \equiv 0$) it is only necessary to solve Laplace's equation on each side of the flame sheet, whence

$$\left.\begin{aligned} &T = T_\mathrm{f} + (T_* - T_\mathrm{f})\frac{r_*}{r}, \quad Y = Y_\mathrm{f}\left(1 - \frac{r_*}{r}\right) \quad (r > r_*), \\ &T = T_*, \quad Y = 0 \quad (r < r_*), \end{aligned}\right\} \tag{2.6}$$

where, apart from boundary conditions, we have only used the continuity of $T$ and

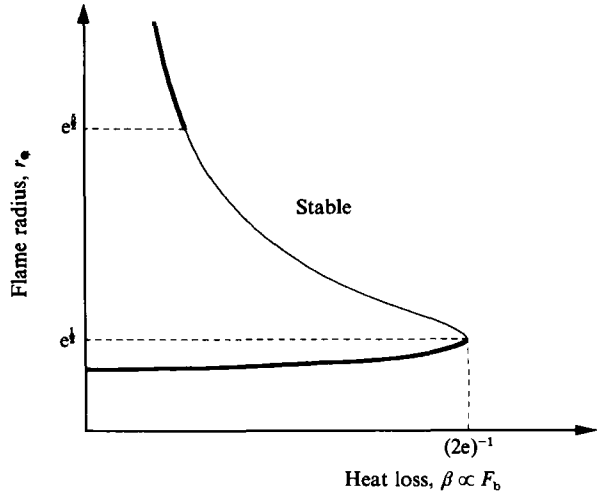


FIGURE 1. Flame-ball radius *vs.* near-field heat loss, $1 = r_* \exp(-\beta r_*^2)$, see Buckmaster *et al.* (1990). The thin line denotes stable solutions.

$Y$ at the flame sheet. The temperature $T_*$ and flame radius $r_*$ are then determined by invoking the gradient conditions (2.4):

$$\left.\begin{aligned} T_* = T_b \equiv T_f + \frac{QY_f}{C_p}\frac{1}{Le}, \quad Le = \frac{\lambda}{\rho D C_p}, \\ r_* = R_z \equiv (\rho D)\frac{Y_f}{B} e^{E/2RT_b}. \end{aligned}\right\} \tag{2.7}$$

$T_b$ may be compared to the adiabatic flame temperature $T_a \equiv T_f + QY_f/C_p$ generated by the propagation of a plane flame. Since $Le$ is small, $T_b$ is substantially larger than $T_a$. $R_z$ is the Zeldovich radius.

This solution is at the core of any discussion of flame balls. All of the solutions that have been constructed, including those in the present paper, are generated by adding various perturbation terms that vanish in the limit $\theta \to \infty$ where $\theta \equiv EC_p/RQ$ is a non-dimensional activation energy. These generate $O(T_b/\theta)$ changes in $T_*$ and $O(R_z)$ changes in $r_*$. For example, Buckmaster *et al.* (1990) accounts for $O(1/\theta)$ radiation losses in the burnt gas and leads to the response of figure 1. In this figure, the Zeldovich solution corresponds to $\beta \to 0$ (vanishing heat loss), $r_*$ finite, and is unstable. For non-vanishing heat losses however, stable solutions are possible, and these are candidates for the experimentally observed flame balls.

The radiation losses of Buckmaster *et al.* (1990) are near-field losses, losses that occur in the region $r = O(R_z)$. Buckmaster *et al.* (1991) examines far-field radiation losses, losses in the region $r = O(\theta R_z)$. The far-field solution controlled by these losses, when matched with the inner solution on the scale $r = O(R_z)$, leads to $O(T_b/\theta)$ changes in $T_*$ and the response shown in figure 2. In related, as yet unpublished work, we have shown that placing a cold wall (at which $T = T_f$) at a distance $O(\theta R_z)$ from the ball also leads to the response of figure 2 ($\alpha$ is then proportional to the inverse of the ball–wall spacing).

These various results suggest that perturbations that modify the Zeldovich solution by extracting heat have a dual effect. If the losses are too large ($\beta > (2e)^{-1}$ in figure 1; $\alpha > e^{-1}$ in figure 2) there is no stationary solution and quenching occurs.

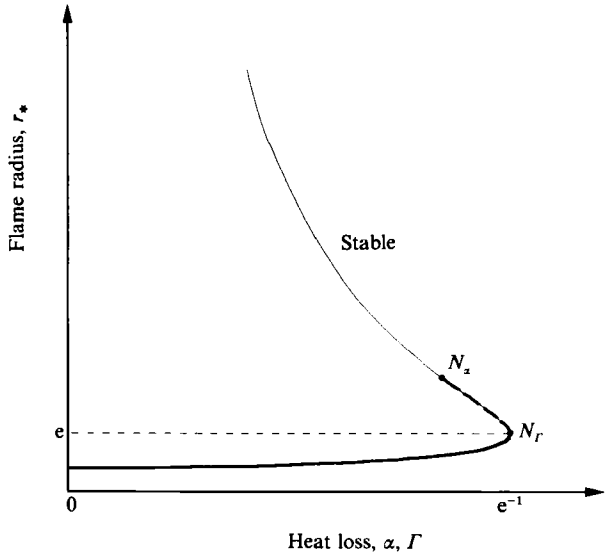


FIGURE 2. Flame-ball radius *vs.* far-field heat loss $\alpha$ (Buckmaster *et al.* 1991), $\Gamma$ (eqn. (3.27)). $N_\alpha$ is the neutral-stability point for radiation losses ($\alpha$); $N_\Gamma$ is the neutral-stability point for convection losses ($\Gamma$).

For losses less than the quenching values, stable stationary solutions are possible. Here we are concerned with the extraction of heat by convection.

The significance of the far field, $r = O(\theta R_z)$, has already been noted, and in the far-field $\nabla^2 \sim 1/\theta^2 R_z^2$. It should be no surprise, therefore, that a slow timescale for which $t \propto \theta^2$ plays an important role: for then, in the far field, the time derivatives are comparable to the Laplacian, and the transient storage of energy can lead to transient fluctuations in $T_*$ of $O(T_b/\theta)$. Indeed, one-dimensional instabilities evolve on this slow time and are responsible for the unstable nature of the lower branches in figures 1 and 2.

Three-dimensional instabilities are responsible for the upper unstable region marked in figure 1 and these also evolve on a slow timescale, but one for which $t \propto \theta$. This emerges from the analysis of Buckmaster *et al.* (1990) and we know of no simple *a priori* demonstration of this fact.

### 2.2. *Non-dimensional variables*

We use $R_z$ (the Zeldovich radius) as the reference length everywhere except in §4. The non-dimensional activation energy is

$$\theta = \frac{EC_p}{RQ} \gg 1; \tag{2.8}$$

and other non-dimensional quantities are

$$\left.\begin{aligned} &\bar{x} = \theta X = \frac{1}{R_z} x, \quad \mathscr{T} = \theta \tau = \frac{\lambda t}{\rho_f C_p R_z^2 \theta}, \\ &\bar{v} = \theta V = \frac{\theta^2 \rho_f R_z C_p}{\lambda} v, \quad P = \theta \bar{p} = \frac{\theta^2 R_z^2 C_p^2 \rho_f}{\lambda^2} p, \\ &\bar{\rho} = \frac{\rho}{\rho_f}, \quad \bar{T} = \frac{C_p T}{Q}, \quad \bar{B} = \frac{R_z C_p}{\lambda} B, \quad F = \frac{\theta R_z^2 C_p}{\lambda Q} f, \quad \bar{\delta} = R_z \delta, \quad \bar{r}_* = \frac{r_*}{R_z}. \end{aligned}\right\} \tag{2.9}$$

The multiple choices simply reflect the fact that different variables are appropriate accordingly as we describe the near field or the far field, and one- or three-dimensional perturbations to the flame sheet. Only in §4 is the latter of concern and so until then the discussion assumes one-dimensional flame-sheet perturbations. Then the appropriate timescale is $\tau(t \propto \theta^2)$.

Far-field variables are $\boldsymbol{X}(\boldsymbol{x} \propto \theta)$, $V(v \propto \theta^{-1})$, $P(p \propto \theta^{-2})$; near-field variables $\bar{\boldsymbol{x}}(\boldsymbol{x} \propto \theta^0)$, $\bar{\boldsymbol{v}}(\boldsymbol{v} \propto \theta^{-2}), P$. An appropriate definition of the Péclet number, a measure of the ratio of convection terms to diffusion terms in the near field, is then

$$Pe = \frac{\rho_f R_z^2 \omega}{\rho D}, \tag{2.10}$$

where $\omega$ is a dimensional velocity gradient characteristic of the applied outer flow. Since $\omega$ is of order $\lambda/(\theta^2 \rho_f R_z^2 C_p)$, $Pe$ is of order $(1/\theta^2)$. As noted in §1, the incremental fluxes arising from convection are proportional to $(Pe)^{\frac{1}{2}}$ so that these are $O(1/\theta)$ and play as important a role as the $O(1/\theta)$ radiation losses ($f \propto \theta^{-1}$). This motivates the scaling that defines $V$.

### 2.3. *The far-field equations and the applied velocity field*

We are concerned with the response of the flame ball to linear shear and straining flows, and to see how these are to be imposed it is necessary to examine the far-field equations. In the far field it is appropriate to write

$$\bar{T} = \bar{T}_f + \frac{1}{\theta} T_1 + \ldots, \quad Y = Y_f + \frac{1}{\theta} Y_1 + \ldots, \quad \bar{\rho} = 1 + \ldots \tag{2.11}$$

so that the continuity equation

$$\frac{\partial \bar{\rho}}{\partial \tau} + \nabla_R \cdot (\bar{\rho} \bar{\boldsymbol{v}}) = 0, \quad \nabla_R \equiv \left( \frac{\partial}{\partial X_1}, \frac{\partial}{\partial X_2}, \frac{\partial}{\partial X_3} \right) \tag{2.12}$$

is, to leading order,

$$\nabla_R \cdot \bar{\boldsymbol{v}} = 0. \tag{2.13}$$

The momentum equation simplifies to

$$\frac{\mathrm{D}\bar{\boldsymbol{v}}}{\mathrm{D}\tau} = -\nabla_R P + Pr \nabla_R^2 \bar{\boldsymbol{v}}, \tag{2.14}$$

$$\frac{\mathrm{D}}{\mathrm{D}\tau} \equiv \frac{\partial}{\partial \tau} + \bar{\boldsymbol{v}} \cdot \nabla_R,$$

where $Pr\,(=\mu C_p/\lambda)$ is the Prandtl number. Thus, provided the near field generates no significant flow (a matter examined below), any suitable solution of the constant-density Navier–Stokes equations can be chosen for the flow field provided that the velocity vanishes as $R = |\boldsymbol{X}| \to 0$ where the flame ball is located. We shall consider linear steady flows only.

$T_1$ and $Y_1$ satisfy the equations

$$\frac{\mathrm{D}T_1}{\mathrm{D}\tau} = \nabla_R^2 T_1, \quad \frac{\mathrm{D}Y_1}{\mathrm{D}\tau} = \frac{1}{Le} \nabla_R^2 Y_1. \tag{2.15}$$

### 2.4. *The near-field equations*

Terms that are $O(1/\theta^2)$ in the near field need never be considered ($O(1/\theta)$ terms play a profound role, however, because of the sensitivity that arises from the Arrhenius' factor). Thus, neglecting $O(1/\theta^2)$ terms, the near-field equations are

$$\left.\begin{aligned} 0 &= \nabla_{\bar{r}}^2 \bar{T} + \bar{B}\,\mathrm{e}^{-\theta/2\bar{T}_*}\bar{\delta} - \frac{1}{\theta}F, \quad \nabla_{\bar{r}} \equiv \left(\frac{\partial}{\partial \bar{x}_1}, \frac{\partial}{\partial \bar{x}_2}, \frac{\partial}{\partial \bar{x}_3}\right), \\ 0 &= \frac{1}{Le}\nabla_{\bar{r}}^2 Y - \bar{B}\,\mathrm{e}^{-\theta/2\bar{T}_*}\bar{\delta}, \quad \bar{\rho}\bar{T} = \bar{T}_{\mathrm{f}}, \\ \frac{\partial \bar{\rho}}{\partial \tau} + \nabla_{\bar{r}}\cdot(\bar{\rho}\bar{v}) &= 0, \quad 0 = -\nabla_{\bar{r}} P + Pr[\nabla_{\bar{r}}^2 \bar{v} + \tfrac{1}{3}\nabla_{\bar{r}}(\nabla_{\bar{r}}\cdot\bar{v})]. \end{aligned}\right\} \tag{2.16}$$

Recall that, by choice, $F$ is only non-zero in the burnt gas.

We are concerned only with spherically symmetric solutions for $\bar{T}$, $Y$ and $\bar{\rho}$. (Asymmetry in the far field does not destroy the symmetry in the near field up to and including $O(1/\theta)$ terms.) Moreover these equations are linear in $\bar{v}$ which can, accordingly, be written as

$$\bar{v} = \bar{v}_{\mathrm{s}} + \bar{v}_{\mathrm{u}}, \tag{2.17}$$

where $\bar{v}_{\mathrm{s}}$ is the extension of the steady far field into the near field (modified by the density changes), and $\bar{v}_{\mathrm{u}}$ is the unsteady radial velocity generated by the temporal density variations. Thus

$$(\bar{v}_{\mathrm{u}})_{\bar{r}} = \frac{-\int_0^{\bar{r}} \mathrm{d}s\, s^2 \dfrac{\partial \bar{\rho}}{\partial \tau}}{\bar{\rho}\bar{r}^2} = \frac{\bar{T}_{\mathrm{f}} \displaystyle\int_0^{\bar{r}} \mathrm{d}s\, s^2 \frac{1}{\bar{T}^2}\frac{\partial \bar{T}}{\partial \tau}}{\bar{\rho}\bar{r}^2}, \tag{2.18}$$

$$\bar{r} = |\bar{x}|.$$

Since, to leading order in the unburnt gas (cf. (2.6)),

$$\bar{T} = \bar{T}_{\mathrm{f}} + (\bar{T}_{\mathrm{b}} - \bar{T}_{\mathrm{f}})\frac{\bar{r}_*}{\bar{r}} \tag{2.19}$$

then

$$(\bar{v}_{\mathrm{u}})_{\bar{r}} \propto \dot{\bar{r}}_* \quad \text{as} \quad \bar{r} \to \infty, \tag{2.20}$$

which generates $O(1/\theta)$ variations in $V$ in the far field, and so is of no consequence.

## 3. Solution for a spherical flame ball

In this section we construct solutions in the near field and far field, and match them to generate steady solutions for a flame ball in a linear shear or straining flow. We also consider the linear stability of these solutions to one-dimensional (spherical) disturbances.

### 3.1. *The fundamental equation for the flame-ball radius*

Examination of the near field enables us to construct an equation for $\bar{r}_*$ that contains only prescribed parameters and a single time-dependent variable that is a characteristic of the far-field solution. This is the fundamental equation for the flame-ball radius.

Equations (2.16) for $\bar{T}$ and $Y$ can be solved in a straightforward fashion. With the flame sheet located at

$$\bar{r} = \bar{r}_*(\tau) \tag{3.1}$$

we have, in $\bar{r} < \bar{r}_*$,

$$\left.\begin{aligned} Y = 0, \quad \bar{T} &= \bar{T}_b + \frac{1}{\theta}[K + \tfrac{1}{6}\bar{r}^2 F_b] + \ldots, \\ \bar{T}_b &= \bar{T}_f + \frac{Y_f}{Le}, \quad F_b = F(\bar{T}_b) \end{aligned}\right\} \tag{3.2}$$

where $K$ is a constant to be determined.

The solution in $\bar{r} > \bar{r}_*$ is

$$\left.\begin{aligned} \bar{T} &= \bar{T}_f + \frac{1}{\theta}A_1 + \left(\frac{Y_f}{Le} + \frac{1}{\theta}D_1\right)\frac{\bar{r}_*}{\bar{r}} + \ldots, \\ Y &= Y_f + \frac{1}{\theta}B_1 + \left(-Y_f + \frac{1}{\theta}E_1\right)\frac{\bar{r}_*}{\bar{r}} + \ldots, \end{aligned}\right\} \tag{3.3}$$

where the matching conditions at infinity and continuity at the flame sheet have both been used to first order. Second-order continuity at the sheet requires

$$B_1 + E_1 = 0, \quad A_1 + D_1 = K + \tfrac{1}{6}\bar{r}_*^2 F_b. \tag{3.4}$$

The jump condition (cf. (2.4))

$$\left[\frac{d\bar{T}}{d\bar{r}}\right] + \frac{1}{Le}\left[\frac{dY}{d\bar{r}}\right] = 0 \tag{3.5}$$

requires

$$D_1 + \frac{E_1}{Le} + \tfrac{1}{3}\bar{r}_*^2 F_b = 0. \tag{3.6}$$

And the condition

$$\left[\frac{dY}{d\bar{r}}\right] = \left.\frac{dY}{d\bar{r}}\right|_{\bar{r}_*+0} = Le\,\bar{B}\,e^{-\theta/2\bar{T}_*}, \tag{3.7}$$

where

$$\frac{\theta}{2\bar{T}_*} = \frac{\theta}{2\bar{T}_b} - \frac{(K + \frac{1}{6}\bar{r}_*^2 F_b)}{2\bar{T}_b^2} + O\left(\frac{1}{\theta}\right), \tag{3.8}$$

leads to

$$1 = \frac{Y_f\, e^{\theta/2\bar{T}_b}}{Le\,\bar{B}} = \bar{r}_* \exp\left(\frac{K + \frac{1}{6}\bar{r}_*^2 F_b}{2\bar{T}_b^2}\right). \tag{3.9}$$

The first formula in (3.9) follows from the fact that $\bar{r}_* = 1$ (the flame radius equals the Zeldovich radius) when $\bar{T}_* = \bar{T}_b$ and there are no heat losses; since $\bar{B}$ is proportional to $R_z$ this recaptures the formula (2.7*b*) for the Zeldovich radius.

Using (3.4) and (3.6), (3.9) can be written as

$$1 = \bar{r}_* \exp\left[\frac{h - \frac{1}{3}\bar{r}_*^2 F_b}{2\bar{T}_b^2}\right], \tag{3.10}$$

where

$$h = A_1 + \frac{B_1}{Le}. \tag{3.11}$$

Note that

$$\bar{T} + \frac{1}{Le}Y = \bar{T}_b + \frac{1}{\theta}h + \ldots. \tag{3.12}$$

Since $h$ can be determined by matching with the outer solution, (3.10) is the fundamental equation that determines $\bar{r}_*$, both for steady and unsteady problems. For example, for steady combustion with no far-field losses, $h = 0$ and (3.10) is the result from Buckmaster *et al.* (1990) shown in figure 1 with $\beta \equiv F_b/6\bar{T}_b^2$.

### 3.2. *Steady solutions*

In general, the variable $h$ in the fundamental equation (3.10) does not vanish, and in this section we calculate it when the far-field velocity is linear.

The far-field perturbations $T_1$ and $Y_1$ satisfy (2.15) which must be solved subject to the following boundary and matching conditions:

$$\left.\begin{aligned} &T_1 \to \frac{Y_f \bar{r}_*}{Le\, R} + \Delta T_1 + o(1), \quad Y_1 \to -Y_f \frac{\bar{r}_*}{R} + \Delta Y_1 + o(1) \quad \text{as} \quad R \to 0, \\ &h = \Delta T_1 + \frac{1}{Le}\Delta Y_1; \\ &T_1 \to 0, \quad Y_1 \to 0 \quad \text{as} \quad R \to \infty. \end{aligned}\right\} \tag{3.13}$$

The flame ball acts as a point source of heat and a point sink of mixture each with a strength proportional to $\bar{r}_*$.

The boundary-value problems for $T_1$ and $Y_1$ are of the form

$$\left.\begin{aligned} &\frac{\partial C}{\partial \tau} + \boldsymbol{V}\cdot\boldsymbol{\nabla}_R C = \kappa \nabla_R^2 C, \\ &C \to \frac{Q}{4\pi\kappa R} + \Delta C + o(1) \quad \text{as} \quad R \to 0, \\ &C \to 0 \quad \text{as} \quad R \to \infty, \end{aligned}\right\} \tag{3.14}$$

where for the linear velocity fields of interest

$$V_i = G_{ij} X_j, \tag{3.15}$$

a solution of (2.13), (2.14).

The goal is to calculate $\Delta C$, and for this we turn to the discussion of Batchelor (1979).

Defining the Fourier transform

$$\hat{C}(\boldsymbol{k}, \tau) = \int e^{-i\boldsymbol{k}\cdot\boldsymbol{X}} C(\boldsymbol{X}, \tau)\, d\boldsymbol{X}, \tag{3.16}$$

the solution for an *instantaneous* point source of strength $Q_0$ is

$$\hat{C} = Q_0 \exp(-\kappa k_i k_j B_{ij}), \tag{3.17}$$

where the symmetric tensor $B_{ij}$ is a function of $\tau$ and satisfies the initial-value problem

$$\left.\begin{aligned} &\frac{dB_{ij}}{d\tau} = \delta_{ij} + G_{il} B_{jl} + G_{jl} B_{il}, \\ &B_{ij} \sim \delta_{ij}\tau \quad \text{as} \quad \tau \to 0. \end{aligned}\right\} \tag{3.18}$$

The steady solution for a source of fixed strength $Q$ is found by integrating (3.17) so that

$$\hat{C} = Q \int_0^\infty d\tau \exp(-\kappa k_i k_j B_{ij}), \tag{3.19}$$

$$\left.\begin{aligned} &\text{and inversion yields} \quad C = \frac{Q}{4\pi\kappa R} + J \\ &\text{where} \quad J = \frac{Q}{(4\pi\kappa)^{\frac{3}{2}}}\int_0^\infty \mathrm{d}\tau \exp\left(\frac{-R^2}{4\kappa\tau}\right)\left\{\frac{1}{D^{\frac{1}{2}}}\exp\left(\frac{R^2}{4\kappa\tau} - \frac{X_i X_j b_{ij}}{4\kappa D}\right) - \frac{1}{\tau^{\frac{3}{2}}}\right\}. \end{aligned}\right\} \tag{3.20}$$

Here $D$ is the determinant of the matrix $\boldsymbol{B}$ and $b_{ij}$ is the cofactor of the matrix element $B_{ij}$.

In order to calculate $\Delta C$ we evaluate $J$ at the origin, whence

$$\Delta C = \frac{Q}{(4\pi\kappa)^{\frac{3}{2}}}\int_0^\infty \mathrm{d}\tau (D^{-\frac{1}{2}} - \tau^{-\frac{3}{2}}). \tag{3.21}$$

Some specific linear flows will now be considered.

*Linear shear*

In the case of simple shear

$$\boldsymbol{V} = (\gamma X_2, 0, 0), \tag{3.22}$$

$D$ is given by the formula

$$D = \tau^3(1 + \tfrac{1}{12}\gamma^2\tau^2), \tag{3.23}$$

so that

$$\Delta C = \frac{Q\gamma^{\frac{1}{2}}}{(4\pi\kappa)^{\frac{3}{2}}}\int_0^\infty \frac{\mathrm{d}q}{q^{\frac{3}{2}}}[(1 + \tfrac{1}{12}q^2)^{-\frac{1}{2}} - 1]$$

$$= -\frac{Q\gamma^{\frac{1}{2}}}{4\pi\kappa^{\frac{3}{2}}}\sigma_1, \quad \sigma_1 = 0.257\ldots. \tag{3.24}$$

Thus $T_1$ and $Y_1$ have the behaviour

$$\left.\begin{aligned} T_1 &= \frac{Y_f \bar{r}_*}{Le\, R} - \frac{Y_f \bar{r}_*}{Le}\gamma^{\frac{1}{2}}\sigma_1 + \ldots, \\ Y_1 &= -\frac{Y_f \bar{r}_*}{R} + Y_f \bar{r}_*(\gamma Le)^{\frac{1}{2}}\sigma_1 + \ldots \quad \text{as} \quad R \to 0 \end{aligned}\right\} \tag{3.25}$$

and

$$h = -Y_f \frac{\gamma^{\frac{1}{2}}\sigma_1}{Le}(1 - (Le)^{\frac{1}{2}})\bar{r}_*. \tag{3.26}$$

If the Lewis number is equal to unity the thermal energy removed by convection is balanced by the energy addition associated with an increased flux of $Y$, and $h$ vanishes. But, for $Le < 1$, $h$ is negative corresponding to net energy removal. $h$ is proportional to $(1 - (Le)^{\frac{1}{2}})$ because the convective fluxes vary as the square-root of the Péclet number.

When the volumetric heat losses are neglected ($F_b = 0$), (3.10) now becomes

$$1 = \bar{r}_* \mathrm{e}^{-\Gamma \bar{r}_*}, \quad \Gamma = \frac{Y_f \gamma^{\frac{1}{2}}\sigma_1[1 - (Le)^{\frac{1}{2}}]}{2\bar{T}_b^2 Le}. \tag{3.27}$$

This equation determines how the radius of the flame varies with the shear $\gamma$ (figure 2). If $\Gamma > \mathrm{e}^{-1}$ quenching occurs, and for smaller values of $\Gamma$ there are two possible solutions. The picture is similar to that of figure 1, the linear dependence of $h$ on $\bar{r}_*$ creating some minor differences. The stability of these solutions is considered later.

*Plane strain*

Here

$$\boldsymbol{V} = E_1(X_1, -X_2, 0), \quad E = \sqrt{2}|E_1|, \tag{3.28}$$

whence
$$D = \frac{2\tau}{E^2}\sinh^2\left(\frac{E\tau}{\sqrt{2}}\right), \tag{3.29}$$

and
$$\Delta C = \frac{QE^{\frac{1}{2}}}{(4\pi\kappa)^{\frac{3}{2}}}\int_0^\infty \mathrm{d}q\left[\frac{1}{(2q)^{\frac{1}{2}}\sinh\dfrac{q}{\sqrt{2}}} - \frac{1}{q^{\frac{3}{2}}}\right]$$

$$= \frac{-QE^{\frac{1}{2}}\sigma_2}{4\pi\kappa^{\frac{3}{2}}}, \quad \sigma_2 = 0.360\ldots. \tag{3.30}$$

The result is identical to that for simple shear provided we make the substitution
$$\gamma^{\frac{1}{2}}\sigma_1 \to E^{\frac{1}{2}}\sigma_2. \tag{3.31}$$

*Axisymmetric straining motion*

With
$$V = E_1(X_1, X_2, -2X_3), \quad E = \sqrt{6}|E_1|, \tag{3.32}$$

$$D = \frac{1}{2E_1^3}\sinh^2(E_1\tau)\sinh(2E_1\tau) \tag{3.33}$$

and
$$\Delta C = \frac{-QE^{\frac{1}{2}}\sigma_2}{4\pi\kappa^{\frac{3}{2}}}, \tag{3.34}$$

which is identical to the result for plane strain.

All of these flows have the same impact on the flame ball, expressed in figure 2. Heat loss in the far field by radiation or to a cold wall has the same effect – only the precise definition of the heat-loss parameter $\alpha$ varies. In this sense figure 2 is a universal curve. In certain applications (such as the non-uniform flows treated here) $\alpha$ is, in principle, under the control of the experimentalist. The ramifications of this are discussed in §5.

### 3.3. *Stability analysis*

The Zeldovich solution is unstable and the most important characteristic of heat losses is that they can be stabilizing. In this section we examine the one-dimensional stability of the steady solutions described above.

The fundamental equation for the flame-ball radius, (3.10), is correct for the unsteady problem provided that the flame sheet is spherical, and for a linear stability analysis it is appropriate to write it in its linearized form,

$$O = \bar{r}_*' - \frac{1}{3}\frac{F_{\mathrm{b}}\bar{r}_{*0}^2\bar{r}_*'}{\bar{T}_{\mathrm{b}}^2} + \frac{\bar{r}_{*0}h'}{2\bar{T}_{\mathrm{b}}^2}, \tag{3.35}$$

where $\bar{r}_{*0}$ is the stationary radius and $\bar{r}_*'$, $h'$ are perturbations. When $h'$ is determined from an examination of perturbations of the far-field variables $T_1$ and $Y_1$, this equation controls the linear stability. Far-field perturbations are governed by

$$\left.\begin{gathered}\frac{\mathrm{D}T'}{\mathrm{D}\tau} = \nabla_R^2 T', \quad \frac{\mathrm{D}Y'}{\mathrm{D}\tau} = \frac{1}{Le}\nabla_R^2 Y' \\ T' \to \frac{Y_{\mathrm{f}}\bar{r}_*'}{Le\,R} + \Delta T' + \ldots, \quad Y' \to -\frac{Y_{\mathrm{f}}\bar{r}_*'}{R} + \Delta Y' + \ldots \quad \text{as} \quad R \to 0, \\ h' = \Delta T' + \frac{1}{Le}\Delta Y', \\ T' \to 0, \quad Y' \to 0 \quad \text{as} \quad R \to \infty.\end{gathered}\right\} \tag{3.36}$$

It is appropriate to assume that

$$\bar{r}'_* = \epsilon\, e^{\alpha\tau}, \quad \mathrm{Re}\,(\alpha) > 0 \tag{3.37}$$

and then evaluate $\Delta T'$ and $\Delta Y'$ for large $\tau$. This can be done by adapting Batchelor's (1979) method to the problem of a time-dependent source so that once again we consider (3.14) for $C$, now with

$$C \to \frac{Q\, e^{\alpha\tau}}{4\pi\kappa R} + \Delta C + \ldots \quad \text{as} \quad R \to 0, \tau > 0. \tag{3.38}$$

The result (3.19) is then replaced by

$$\hat{C}(\boldsymbol{k}) = Q \int_0^\tau dm\, e^{\alpha(\tau - m)} \exp(-\kappa k_i k_j B_{ij}), \tag{3.39}$$

and upon inversion

$$C = \frac{Q\, e^{\alpha\tau}}{(4\pi\kappa)^{\frac{3}{2}}} \int_0^\tau \frac{dm}{m^{\frac{3}{2}}} \exp\left(-\frac{R^2}{4\kappa m}\right) + \frac{Q\, e^{\alpha\tau}}{(4\pi\kappa)^{\frac{3}{2}}} \int_0^\tau dm \exp\left(-\frac{R^2}{4\kappa m}\right) \times \left\{\frac{e^{-\alpha m}}{D^{\frac{1}{2}}} \exp\left(\frac{R^2}{4\kappa m} - \frac{X_i X_j b_{ij}}{4\kappa D}\right) - \frac{1}{m^{\frac{3}{2}}}\right\}. \tag{3.40}$$

Taking the limit $R \to 0$, and with $\tau$ large, it follows that

$$\Delta C = \frac{Q\, e^{\alpha\tau} S}{(4\pi\kappa)^{\frac{3}{2}}}, \quad S = \int_0^\infty dm \left[\frac{e^{-\alpha m}}{D^{\frac{1}{2}}} - \frac{1}{m^{\frac{3}{2}}}\right], \tag{3.41}$$

and

$$h' = \frac{Y_f \bar{r}'_*}{Le\,(4\pi)^{\frac{1}{2}}} (1 - (Le)^{\frac{1}{2}}) S. \tag{3.42}$$

When this is substituted into (3.35) we arrive at the equation governing the eigenvalue $\alpha$,

$$0 = 1 - \frac{1}{3} \frac{F_b \bar{r}_{*0}^2}{\bar{T}_b^2} + \frac{\bar{r}_{*0} Y_f}{2\bar{T}_b^2 Le (4\pi)^{\frac{1}{2}}} (1 - (Le)^{\frac{1}{2}}) S. \tag{3.43}$$

We now set $F_b = 0$, neglecting volumetric heat losses, and deduce the stability consequences for simple shear and strain.

*Linear shear*

Referring to (3.22), (3.23), $S$ is defined by

$$S = \int_0^\infty \frac{dm}{m^{\frac{3}{2}}} \left[\frac{e^{-\alpha m}}{(1 + \frac{1}{12}\gamma^2 m^2)^{\frac{1}{2}}} - 1\right]. \tag{3.44}$$

It is immediately clear that the only roots of (3.43) are real, for if $\alpha = \alpha_r + i\alpha_i$ it is necessary that

$$\int_0^\infty \frac{dm}{m^{\frac{3}{2}}} \frac{e^{-\alpha_r m} \sin \alpha_i m}{(1 + \frac{1}{12}\gamma^2 m^2)^{\frac{1}{2}}} = 0 \tag{3.45}$$

and since, apart from the factor $\sin \alpha_i m$, the integrand is a monotone decreasing function of $m$, this condition can only be satisfied if $\alpha_i = 0$.

The neutral stability point ($\alpha = 0$) is located at $\bar{r}_{*0} = \Gamma^{-1}$ (the quenching point) and $\alpha > 0$ for $\bar{r}_{*0} < \Gamma^{-1}$. Thus the entire lower branch of figure 2 is unstable.

*Simple strain*

Here also, for both plane and axisymmetric strain, there are no complex roots and instability is predicted for the lower branch (only).

For all of these flows the one-dimensional stability analysis leaves all points on the upper branch ($\bar{r}_* > \mathrm{e}$) as candidates for physically realizable flame balls.

## 4. Three-dimensional stability analysis

In this section we consider disturbances to the stationary solution characterized by corrugations of the flame sheet. The analysis is quite complicated, but has two motivations. First, it is shown in Buckmaster *et al.* (1990) that three-dimensional instabilities restrict the range of stable solutions on the upper branch (see figure 1, instability for $\bar{r}_* > \mathrm{e}^{\frac{5}{2}}$), a possibility here also. And second, the analysis of Buckmaster *et al.* (1990) is based on the constant-density model (eliminating induced hydrodynamic disturbances) and here we avoid that assumption. Thus the present analysis contains, as a special case ($Pe \to 0$), a correct analysis for the flames of Buckmaster *et al.* (1990).

Consider the equations that govern the near field. As noted earlier, the correct timescale is $\mathscr{T}$ ($t \propto \theta$). Correspondingly the flow scalings are different from those appropriate for one-dimensional disturbances: we use $V(v \propto \theta^{-1})$ and $\bar{p}(p \propto \theta^{-1})$. Then,

$$\left.\begin{gathered}\frac{1}{\theta}\bar{\rho}\frac{\mathrm{D}\bar{T}}{\mathrm{D}\mathscr{T}} = \bar{\nabla}^2\bar{T} + \bar{B}\,\mathrm{e}^{-\theta/2\bar{T}_*}\bar{\delta} - \frac{F}{\theta}, \quad \frac{\mathrm{D}}{\mathrm{D}\mathscr{T}} = \frac{\partial}{\partial\mathscr{T}} + \boldsymbol{V}\cdot\bar{\boldsymbol{\nabla}}, \\ \frac{1}{\theta}\bar{\rho}\frac{\mathrm{D}Y}{\mathrm{D}\mathscr{T}} = \frac{1}{Le}\bar{\nabla}^2 Y - \bar{B}\,\mathrm{e}^{-\theta/2\bar{T}_*}\bar{\delta}, \quad \bar{\rho}\bar{T} = \bar{T}_{\mathrm{f}}, \\ \frac{\partial\bar{\rho}}{\partial\mathscr{T}} + \bar{\boldsymbol{\nabla}}\cdot(\bar{\rho}\boldsymbol{V}) = 0, \quad \frac{1}{\theta}\bar{\rho}\frac{\mathrm{D}\boldsymbol{V}}{\mathrm{D}\mathscr{T}} = -\bar{\boldsymbol{\nabla}}\bar{p} + Pr[\bar{\nabla}^2\boldsymbol{V} + \tfrac{1}{3}\bar{\boldsymbol{\nabla}}(\bar{\boldsymbol{\nabla}}\cdot\boldsymbol{V})].\end{gathered}\right\} \tag{4.1}$$

These equations are unchanged in form if a lengthscale different from $R_z$ is used; and the relative magnitude of terms is unchanged if the new length is comparable to $R_z$. It is convenient to use the steady radius $R_0$ as the reference length, and then the undisturbed flame sheet is located at $\bar{r}_* = 1$.

We consider perturbations to the flame sheet in the form of surface harmonics,

$$\bar{r}_* = 1 + \epsilon\mathbb{P}, \quad \mathbb{P} = \mathrm{e}^{\mathrm{i}m\phi}P_n^m(x)\,\mathrm{e}^{\alpha\mathscr{T}}, \quad n \geqslant m, \quad x = \cos\theta, \tag{4.2}$$

where $\theta, \phi$ are angular coordinates.

We record here the stationary solution for a simple shear (for a simple strain replace $\gamma^{\frac{1}{2}}\sigma_1$ by $E^{\frac{1}{2}}\sigma_2$):

$$\left.\begin{gathered}Y = 0, \quad \bar{T} = \bar{T}_{\mathrm{b}} + \frac{1}{\theta}\left[-\tfrac{1}{2}F_{\mathrm{b}} - Y_{\mathrm{f}}\frac{\gamma^{\frac{1}{2}}\sigma_1}{Le}(1-(Le)^{\frac{1}{2}}) + \tfrac{1}{6}\bar{r}^2F_{\mathrm{b}}\right] + \ldots \quad (\bar{r} < 1), \\ Y = Y_{\mathrm{f}}\left(1 - \frac{1}{\bar{r}}\right) + \frac{1}{\theta}\left[Y_{\mathrm{f}}(\gamma Le)^{\frac{1}{2}}\sigma_1 - Y_{\mathrm{f}}(\gamma Le)^{\frac{1}{2}}\frac{\sigma_1}{\bar{r}}\right] + \ldots, \\ \bar{T} = \bar{T}_{\mathrm{f}} + \frac{Y_{\mathrm{f}}}{Le}\frac{1}{\bar{r}} + \frac{1}{\theta}\left[-Y_{\mathrm{f}}\frac{\gamma^{\frac{1}{2}}}{Le}\sigma_1 + \frac{1}{\bar{r}}\left(-\tfrac{1}{3}F_{\mathrm{b}} + Y_{\mathrm{f}}\frac{(\gamma Le)^{\frac{1}{2}}}{Le}\sigma_1\right)\right] + \ldots \quad (\bar{r} > 1),\end{gathered}\right\} \tag{4.3}$$

where the stationary radius $R_0$ is determined by the equation

$$Y_f = Le\bar{B}\,e^{-\theta/2\bar{T}_b}\exp\left[\frac{-\frac{1}{3}F_b - Y_f\gamma^{\frac{1}{2}}\dfrac{\sigma_1}{Le}(1-(Le)^{\frac{1}{2}})}{2\bar{T}_b^2}\right], \tag{4.4}$$

bearing in mind that now $\bar{B}$, $F_b$ and $\gamma$ all depend on $R_0$.

Consider infinitesimal perturbations to the stationary solution $\bar{T}_0, \bar{\rho}_0$, etc. These satisfy the following equations:

for $r \in [0, r_*) \cup (r_*, \infty)$ (i.e. excluding the flame-sheet)

$$\frac{1}{\theta}\bar{\rho}_0(\alpha T' + \boldsymbol{V}'\cdot\bar{\boldsymbol{\nabla}}\bar{T}_0) = \bar{\nabla}^2 T' - \frac{F'(\bar{T}_0)\,T'}{\theta}, \tag{4.5a}$$

$$\frac{1}{\theta}\bar{\rho}_0(\alpha Y' + \boldsymbol{V}'\cdot\bar{\boldsymbol{\nabla}}Y_0) = \frac{1}{Le}\bar{\nabla}^2 Y'. \tag{4.5b}$$

for $\bar{r} \in [0, \infty)$

$$\alpha\rho' + \bar{\boldsymbol{\nabla}}\cdot(\bar{\rho}_0\,\boldsymbol{V}') = 0, \quad \rho' = -\frac{\bar{T}_f'}{\bar{T}_0^2}T', \tag{4.6a, b}$$

$$\frac{\alpha}{\theta}\bar{\rho}_0\,\boldsymbol{V}' = -\bar{\boldsymbol{\nabla}}p' + Pr[\bar{\nabla}^2\boldsymbol{V}' + \tfrac{1}{3}\bar{\boldsymbol{\nabla}}(\bar{\boldsymbol{\nabla}}\cdot\boldsymbol{V}')]. \tag{4.6c}$$

### 4.1. *Some preliminaries*

Taking the curl of the momentum equation (4.6*c*) yields

$$\frac{\alpha}{\theta}\bar{\boldsymbol{\nabla}}\times(\bar{\rho}_0\,\boldsymbol{V}') = Pr\bar{\nabla}^2(\bar{\boldsymbol{\nabla}}\times\boldsymbol{V}') \tag{4.7}$$

and the left-hand side is small in the near field. For large values of $\bar{r}$ the equation can be approximated by

$$\frac{\alpha}{\theta}\bar{\boldsymbol{\nabla}}\times\boldsymbol{V}' = Pr\bar{\nabla}^2(\bar{\boldsymbol{\nabla}}\times\boldsymbol{V}') \tag{4.8}$$

where both terms are comparable when $\bar{r} = O(\theta^{\frac{1}{2}})$ (a 'far-field' insofar as three-dimensional disturbances are concerned, the structure of which is unimportant and the essential role of which is merely to impose a 'minimum singularity' condition on the solution in the region $\bar{r} = O(1)$). Thus there is no mechanism to generate vorticity to first order, and we may write

$$\boldsymbol{V}' = \bar{\boldsymbol{\nabla}}\phi, \tag{4.9}$$

where $\phi$ is the velocity potential.

Temperature perturbations satisfy Laplaces equation to first order, with solutions

$$T' = \frac{A_1^-}{\theta}\bar{r}^n P^n + \ldots \quad (\bar{r} < 1), \tag{4.10a}$$

$$T' = A_0^+\bar{r}^{-n-1}P^n + \ldots \quad (\bar{r} > 1). \tag{4.10b}$$

We have anticipated that flame-temperature perturbations are $O(1/\theta)$, hence the perturbations in the burnt gas are small. And for $\bar{r} > 1$ we have invoked a *minimum singularity* condition, discarding the solution $\bar{r}^n$ which cannot be matched with a far

field on the scale $\bar{r} = O(\theta^{\frac{1}{2}})$. This kind of choice will be made on several occasions below, and in due course we shall indicate the nature of the solution in this far field.

### 4.2. *The velocity potential*

Consider now the continuity equation (4.6$a$). Writing

$$\phi = \mathbb{P}\Phi(\bar{r}) \tag{4.11}$$

this is

$$\bar{r}^2\Phi'' + \left(2\bar{r} - \frac{\bar{r}^2}{\bar{T}_0}\frac{\mathrm{d}\bar{T}_0}{\mathrm{d}\bar{r}}\right)\Phi' - (n^2+n)\,\Phi = \frac{\alpha\bar{r}^2 T'}{\bar{T}_0\,\mathbb{P}}. \tag{4.12}$$

In $\bar{r} < 1$ this simplifies to

$$\bar{r}^2\Phi'' + 2\bar{r}\Phi' - (n^2+n)\,\Phi = 0 \tag{4.13}$$

to leading order, with solution

$$\Phi = B^-\bar{r}^n. \tag{4.14}$$

This implies that

$$n\Phi = \frac{\mathrm{d}\Phi}{\mathrm{d}\bar{r}} \tag{4.15}$$

on the burnt side of the flame sheet, and this will also be true on the unburnt side since $\phi$ and $V'$ are continuous.

In $\bar{r} > 1$,

$$\bar{r}^2(1+v\bar{r})\,\Phi'' + r(3+2v\bar{r})\,\Phi' - (n^2+n)(1+v\bar{r})\,\Phi = \frac{\alpha A_0^+\bar{r}^{-n+2}}{(\bar{T}_\mathrm{b}-\bar{T}_\mathrm{f})}, \tag{4.16}$$

where

$$v = \frac{\bar{T}_\mathrm{f}}{\bar{T}_\mathrm{b}-\bar{T}_\mathrm{f}}.$$

To solve this equation we write

$$\left.\begin{aligned} &\Phi = \frac{\alpha A_0^+}{\bar{T}_\mathrm{f}\,v^{1-n-m}}\bar{r}^N g(s), \quad s = v\bar{r}, \\ &N = -1+(1+n+n^2)^{\frac{1}{2}}, \quad n = -\tfrac{1}{2}+\tfrac{1}{2}(1+4N^2+8N)^{\frac{1}{2}}, \end{aligned}\right\} \tag{4.17}$$

so that

$$s(1+s)\,g'' + [2N+3+2(1+N)\,s]\,g' - Ng = s^{1-n-N}, \tag{4.18}$$

with the boundary condition (4.15), i.e.

$$-v\frac{\mathrm{d}g}{\mathrm{d}s} = (N-n)\,g \quad \text{at} \quad s = v. \tag{4.19}$$

Moreover,

$$g \to 0 \quad \text{as} \quad s \to \infty \tag{4.20}$$

since the behaviour $s^{n-N}$ is not permitted (for then $\phi \sim \bar{r}^n$).

Define

$$u(s) = \int_0^1 \mathrm{d}t\, t^{N+n}(1-t)^{N-n+1}(1+ts)^{n-N}; \tag{4.21}$$

this hypergeometric function is a solution of the homogeneous equation. Then

$$g = Ku(s)\int_\infty^s \frac{\mathrm{d}t(1+t)}{u^2(t)\,t^{2N+3}} + u(s)\int_\infty^s \frac{\mathrm{d}\tau(1+\tau)}{u^2(\tau)\,\tau^{2N+3}}\int_0^\tau \mathrm{d}t\,\frac{t^{N-n+3}u(t)}{(1+t)^2}, \tag{4.22}$$

where $K$ is a constant determined by the boundary condition (4.19).

### 4.3. *Temperature perturbations in* $\bar{r} > 1$

With the velocity determined we may now calculate corrections to $T'$ in $\bar{r} > 1$. Extending the *ansatz* (4.10*b*)

$$T' = A_0^+ \bar{r}^{-n-1} \mathbb{P} + \frac{\Psi(\bar{r})}{\theta} \mathbb{P} + \ldots, \tag{4.23}$$

where, from (4.5*a*),

$$\bar{r}^2 \Psi'' + 2\bar{r}\Psi' - (n^2+n)\,\Psi = \alpha A_0^+ [P(\bar{r}) + Q(\bar{r})]. \tag{4.24}$$

Here the functions $P$ and $Q$ are defined by

$$P(\bar{r}) = \frac{v\bar{r}}{1+v\bar{r}} \bar{r}^{-n+1}, \quad Q(\bar{r}) = -\frac{v\bar{r}}{1+v\bar{r}} \frac{\bar{r}^N}{v^{2-n-N}} [N\bar{r}^{-1} g(\bar{r}v) + v g'(\bar{r}v)]. \tag{4.25}$$

Since $\Psi \to 0$ as $\bar{r} \to \infty$ (the $\bar{r}^n$ solution is not acceptable), the solution is

$$\Psi = A_1^+ \bar{r}^{-n-1} + \frac{\alpha A_0^+ \bar{r}^n}{1+2n} \int_\infty^{\bar{r}} \mathrm{d}t\, t^{-n-1}(P(t)+Q(t)) - \frac{\alpha A_0^+ \bar{r}^{-n-1}}{1+2n} \int_1^{\bar{r}} \mathrm{d}t\, t^n (P(t)+Q(t)). \tag{4.26}$$

### 4.4. *Solution for* $Y'$

Turning now to (4.5*b*), the solution for $Y'$ in $\bar{r} > 1$ is

$$Y' = C_0 \bar{r}^{-n-1} \mathbb{P} + \frac{\Sigma(\bar{r})}{\theta} \mathbb{P} + \ldots, \tag{4.27}$$

where

$$\bar{r}^2 \Sigma'' + 2\bar{r}\Sigma' - (n^2+n)\,\Sigma = \alpha C_0 Le\, P(\bar{r}) - \frac{\alpha A_0^+ Le\, Y_{\mathrm{f}} v}{\bar{T}_{\mathrm{f}}} Q(\bar{r}). \tag{4.28}$$

This has solution

$$\begin{aligned} \Sigma = {} & C_1 \bar{r}^{-n-1} + \alpha \frac{C_0 Le\, \bar{r}^n}{1+2n} \int_\infty^{\bar{r}} \mathrm{d}r\, r^{-n-1} P(r) - \frac{\alpha A_0^+}{1+2n} \frac{Le\, Y_{\mathrm{f}} v \bar{r}^n}{\bar{T}_{\mathrm{f}}} \int_\infty^{\bar{r}} \mathrm{d}r\, r^{-n-1} Q(r) \\ & - \frac{\alpha C_0 Le}{1+2n} \bar{r}^{-n-1} \int_1^{\bar{r}} \mathrm{d}r\, r^n P(r) + \frac{\alpha A_0^+}{1+2n} \frac{Le\, Y_{\mathrm{f}} v}{\bar{T}_{\mathrm{f}}} \bar{r}^{-n-1} \int_1^{\bar{r}} \mathrm{d}r\, r^n Q(r). \end{aligned} \tag{4.29}$$

From this description of the perturbation structure it is apparent that on the scale $r = O(\theta^{\frac{1}{2}})$ we have, to leading order, the balance

$$\frac{1}{\theta} \alpha T' = \bar{\nabla}^2 T'$$

for which the solution that does not grow exponentially at infinity, involving the Bessel function $K_{n+\frac{1}{2}}$, behaves like $\bar{r}^{-n-1}$ as $\bar{r} \to 0$ and matches with (4.10*b*). The other variables can be discussed in a similar fashion and this justifies the minimum-singularity condition that has been invoked during this discussion.

### 4.5. *The dispersion relation and its consequences*

We have expressed the perturbations $T'$ and $Y'$, correct to $O(1/\theta)$, in terms of the constants $A_1^-, A_0^+, A_1^+, C_0$ and $C_1$. Algebraic equations relating these constants and the amplitude of $r'_*$ (i.e. $\epsilon$) are generated when the connection conditions at the flame

sheet are invoked. These equations are given in the Appendix. The algebraic system is homogeneous and only has a solution if $\alpha$ satisfies the dispersion relation

$$\alpha = \frac{2(n-1)\bar{T}_b^2\left[\frac{1}{3}\frac{F_b}{\bar{T}_b^2} - (2n+1)\right]}{Y_f((Le)^{-1}-1)\int_1^\infty \mathrm{d}r\, r^{-n-1}(P(r)+Q(r))}. \tag{4.30}$$

Numerical evaluation of the integral shows that the denominator is positive. For example, when $n = 2, v = \frac{1}{3}$ we find $K = -0.000236\ldots$ and

$$\int_1^\infty \mathrm{d}r\, r^{-n-1}Q(r) = v^3 0.11\ldots$$

which is positive. The contribution

$$\int_1^\infty \mathrm{d}r\, r^{-n-1}P(r)$$

is positive by inspection. Note that this result does not explicitly contain $\gamma$ – the only role played by the shear is in controlling $R_0$ (contained in $F_b$).

It is useful, in interpreting this result, to identify the connection between dimensional and non-dimensional variables. If the flow is described by

$$\boldsymbol{v} = (\omega x_2, 0, 0) \tag{4.31}$$

so that $\omega$ is a dimensional shear gradient, then

$$\gamma = \frac{\theta^2 \rho_f C_p R_0^2 \omega}{\lambda}. \tag{4.32}$$

Other useful formulae are

$$\left.\begin{aligned} R_z = \frac{\lambda Y_f \mathrm{e}^{-\theta/2\bar{T}_b}}{C_p B Le}, \quad \Gamma = \frac{R_z Y_f \sigma_1 (1-(Le)^{\frac{1}{2}})}{2Le\,\bar{T}_b^2}\theta\left(\frac{\rho_f C_p \omega}{\lambda}\right)^{\frac{1}{2}}, \\ \frac{F_b}{6\bar{T}_b^2} = \frac{\theta C_p f_b R_0^2}{6\bar{T}_b^2 \lambda Q} \equiv \Omega\left(\frac{R_0}{R_z}\right)^2. \end{aligned}\right\} \tag{4.33}$$

Then the steady radius is described by

$$1 = \frac{R_0}{R_z}\exp\left\{-\Omega\left(\frac{R_0}{R_z}\right)^2 - \Gamma\left(\frac{R_0}{R_z}\right)\right\} \tag{4.34}$$

and we have three-dimensional instability if

$$\frac{R_0}{R_z} > \left(\frac{5}{2\Omega}\right)^{\frac{1}{2}} \tag{4.35}$$

corresponding to the choice $n = 2$ in (4.30). This agrees with previous results obtained for $\Gamma = 0$ (zero Péclet number) using the constant-density model (Buckmaster *et al.* 1990). (Note that $\alpha = 0$ when $n = 1$, for this corresponds merely to translation of the flame ball with unchanged shape. Thus $n = 2$ is the smallest value of $n$ for which $\alpha > 0$.)

It follows that if $\Omega = 0$ there is no three-dimensional instability of the type considered here. As $\Gamma$ is reduced along the upper branch ever larger stable flame balls are generated but the flame-temperature is

$$\left.\begin{aligned} \bar{T}_* &= \bar{T}_b - \frac{1}{\theta} Y_f \gamma^{\frac{1}{2}} \sigma_1 \frac{(1-(Le)^{\frac{1}{2}})}{Le} + \dots \\ \text{and} \qquad \gamma^{\frac{1}{2}} &\propto \frac{R_0}{R_z} \Gamma = \ln\left(\frac{R_0}{R_z}\right), \end{aligned}\right\} \tag{4.36}$$

so that the description is not uniformly valid. We have not examined this non-uniformity.

## 5. Concluding remarks

We have shown that extraction of energy by a non-uniform flow field can stabilize flame balls. This is an *extrinsic* agency unlike the radiation losses considered in earlier work. This has two consequences.

When the only heat loss mechanism is *intrinsic* it is to be expected that for a given mixture all flame balls will be equal in size. With *extrinsic* losses the size of each flame ball will depend on the magnitude of the agencies acting upon it. In ignition experiments it is to be expected that each ball will experience a different non-uniform flow, and this provides a plausible explanation for the different sizes that are observed. It would appear that in drop-tower experiments the size distribution tends to be bimodal and whether or not this is consistent with these remarks would require more knowledge of the unsteady flow field than is presently available.

Extrinsic agencies are, in principle, under the control of the experimentalist. This is of little importance in drop-tower experiments, where the test times are so short, or in flight experiments where there is significant g-jitter, but could be of interest in orbital experiments (shuttle or space station).

Amongst other things, controlling losses via a flow field could lead to flame-ball formation in mixtures that do not support them when the only losses are from radiation. To date, flame-ball gases have two characteristics – they have a Lewis number significantly less than unity, and they are near-limit mixtures. If the concentration of the deficient component (e.g. hydrogen in a lean hydrogen/air mixture) lies sufficiently above the limit value, the initial flame kernel generated by the spark forms cells and these separate (because of the small $Le$) but do not close to form balls. It is plausible to associate this failure with the three-dimensional instability of figure 1. Decreasing the mixture strength towards the limit value increases the relative radiation losses ($F_b$ is proportional to $R_z^2$, (2.9), and $R_z$ is proportional to $Y_f e^{E/2RT_b}$, (2.7), so that a decrease in $Y_f$ (and therefore $T_b$) increases $F_b$), and this can eliminate the instability and allow flame-ball formation. Alternatively, increasing the losses by means of an applied flow could also eliminate the instability without a change in mixture strength.

One final remark: the present results lend credence to the suggestion in Weeratunga, Buckmaster & Johnson (1990) that convection stabilizes the flame caps observed at 1g.

The work of John Buckmaster was supported by the Air Force Office of Scientific Research. We are grateful to R. E. Johnson whose broad knowledge of the fluid-mechanics literature spared us many hours in the library. And we note that the title

of our paper is adapted from that of Batchelor (1979), partly to recognize that our task was considerably simplified by the elegant discussion of small-Péclet-number flows contained therein.

## Appendix

The flame-sheet conditions governing three-dimensional perturbations are written here. These are applied at $\bar{r} = \bar{r}_* = 1+\epsilon\mathbb{P}$ whence for example,

$$Y'_* = Y'(\bar{r}=1+0)+\epsilon\mathbb{P}\frac{\mathrm{d}Y_0}{\mathrm{d}\bar{r}}(\bar{r}=1+0). \tag{A 1}$$

This must vanish and evaluation at the $O(1)$ and $O(1/\theta)$ levels yields the formulae

$$C_0+\epsilon Y_\mathrm{f}=0, \tag{A 2}$$

$$C_1+\frac{\alpha C_0 Le}{(1+2n)}\int_\infty^1 \mathrm{d}r\, r^{-n-1}P(r)-\frac{\alpha A_0^+}{1+2n}\frac{Le\,Y_\mathrm{f}\upsilon}{\bar{T}_\mathrm{f}}\int_\infty^1 \mathrm{d}r\, r^{-n-1}Q(r)+Y_\mathrm{f}(\gamma Le)^{\frac{1}{2}}\sigma_1\epsilon=0. \tag{A 3}$$

In a similar fashion continuity of $T$ requires

$$A_0^+-\epsilon\frac{Y_\mathrm{f}}{Le}=0, \tag{A 4}$$

$$A_1^++\frac{\alpha A_0^+}{1+2n}\int_\infty^1 \mathrm{d}r\, r^{-n-1}(P(r)+Q(r))-\epsilon Y_\mathrm{f}\frac{(\gamma Le)^{\frac{1}{2}}}{Le}\sigma_1-A_1^-=0. \tag{A 5}$$

Noting that for infinitesimal perturbations the distinction between the normal and the radial directions is insignificant, the gradient condition (3.5) leads to

$$-(n+1)\frac{C_1}{Le}+\frac{n\alpha C_0}{1+2n}\int_\infty^1 \mathrm{d}r\, r^{-n-1}P(r)-\frac{n\alpha}{1+2n}\frac{A_0^+Y_\mathrm{f}\upsilon}{\bar{T}_\mathrm{f}}\int_\infty^1 \mathrm{d}r\, r^{-n-1}Q(r)$$

$$-(n+1)A_1^++\frac{n\alpha A_0^+}{1+2n}\int_\infty^1 \mathrm{d}r\, r^{-n-1}(P(r)+Q(r))-\epsilon F_\mathrm{b}-nA_1^-=0. \tag{A 6}$$

We have only written the $O(1/\theta)$ result since the $O(1)$ result is redundant. Finally, the condition (3.7) yields

$$-(n+1)C_0-\epsilon 2Y_\mathrm{f}=\frac{Y_\mathrm{f}}{2\bar{T}_\mathrm{b}^2}\left(A_1^-+\epsilon\frac{F_\mathrm{b}}{3}\right). \tag{A 7}$$

Equation (3.7) can only be used at the $O(1)$ level since $\bar{T}_*$ is known only to $O(1/\theta)$.

The six equations (A 2)–(A 6) define a homogeneous system for the constants $A_1^-$, $A_0^+$, $A_1^+$, $C_0$, $C_1$ and $\epsilon$ and this only has a solution if $\alpha$ satisfies the dispersion relation (4.30).

## REFERENCES


Batchelor, G. K. 1979 Mass transfer from a particle suspended in fluid with a steady linear ambient velocity distribution. *J. Fluid Mech.* **95**, 369–400.

Buckmaster, J. D., Joulin, G. & Ronney, P. D. 1990 Structure and stability of non-adiabatic flame-balls. *Combust. Flame* **79**, 381–392.

Buckmaster, J. D., Joulin, G. & Ronney, P. D. 1991 Structure and stability of non-adiabatic flame-balls, II. Effects of far-field losses. *Combust. Flame* (to appear).

BUCKMASTER, J. D. & LUDFORD, G. S. S. 1983 *Lectures on Mathematical Combustion*, p. 22. CBMS-NSF Regional Conference Series in Applied Mathematics, vol. 43. SIAM.

LEWIS, B. & ELBE, G. VON 1987 *Combustion, Flames and Explosions of Gases*, 3rd edn, p. 326. Academic.

RONNEY, P. D. 1990 Near-limit flame structures at low Lewis number. *Combust. Flame* **82**, 1–14.

WEERATUNGA, S., BUCKMASTER, J. & JOHNSON, R. E. 1990 A flame-bubble analogue and its stability. *Combust. Flame* **79**, 100–109.

WILLIAMS, F. A. 1985 *Combustion Theory*, 2nd edn. Benjamin/Cummings.

ZELDOVICH, YA. B., BARENBLATT, G. I., LIBROVICH, V. B. & MAKHVILADZE, G. M. 1985 *The Mathematical Theory of Combustion and Explosions*, p. 327. New York: Consultants Bureau.